Stress relaxation effect on transport properties of strained vanadium dioxide epitaxial thin films

Kazuki Nagashima, Takeshi Yanagida,* Hidekazu Tanaka, and Tomoji Kawai
Institute of Scientific and Industrial Research, Osaka University, 8-1 Mihogaoka, Ibaraki, Osaka 567-0047, Japan
(Received 13 July 2006; revised manuscript received 6 September 2006; published 17 November 2006)

A stress relaxation effect on the transport properties of strained vanadium dioxide epitaxial thin films grown on TiO_2 (001) single crystal was investigated. When varying the film thickness ranging from 10 to 30 nm, there were no significant changes on the crystal structures identified by x-ray diffraction, i.e., no observable stress relaxation effects. On the other hand, increasing the film thickness resulted in the drastic changes on the transport properties including emerging the multisteps of the metal-insulator transition and also increasing the resistivity. The discrepancy between the observed crystal structure and the transport properties was related to the presence of the nanoscale line cracks due to thermal stress. Thus controlling thermal stress relaxation rather than the stress due to the lattice mismatch is critical to investigate the intrinsic nature on the transport properties of strained vanadium dioxide epitaxial thin films.

DOI: 10.1103/PhysRevB.74.172106 PACS number(s): 77.80.Bh, 71.30.+h, 73.50.−h, 74.62.−c

INTRODUCTION

Vanadium dioxide (VO_2) exhibits a metal-insulator transition (MIT) at 341 K, accompanied by the structural change from a high-temperature tetragonal structure (metal) to a low-temperature monoclinic structure (insulator).[1–6] The MIT in VO_2 has attracted much attention due to not only the intriguing nature as to the roles of the electron correlations and the structural distortions but also the potential applications including switching devices and sensors working at room temperature (RT).[7–17] Controlling arbitrarily the MIT temperature by external stimuli is an interesting issue in terms of the fundamental physics and also the practical applications. One of powerful ways in modifying the MIT temperature is applying a stress, which results in the variation of V-V chain length, since the V-V chain along the *c* axis plays an important role on the charge transfer in the metal phase.[18–20] For instance, applying a hydrostatic pressure to a bulk single crystal was found to be effective to modulate the MIT temperature.[18] More recently, it was found that strained VO_2 thin films grown on a TiO_2 (001) substrate, in which the films received a tensile strain along the in-plane axis with the lattice mismatch 0.863%, exhibited the MIT temperature near RT.[19,20] The modulation of the MIT temperature in the strained thin films is rather drastic, even compared with results of hydrostatic pressure experiments. Since generally such strain effects in oxide thin films strongly depend on the relaxation with increasing the film thickness,[21,22] understanding such relaxation effects is essential to investigate the intrinsic nature in the physical properties of the strained oxide thin films. As far as we are aware, there are no previous reports concerned with the relaxation effects on the strained VO_2 thin films. Here we present an experimental investigation in the context with the stress relaxation effects on the transport properties of strained VO_2 thin films.

EXPERIMENTS

VO_2 films were grown epitaxially on TiO_2 (001) single crystal substrate by pulsed laser deposition (ArF excimer, $\lambda = 193$ nm) at 1 Pa of the oxygen pressure and 643 K of the substrate temperature during deposition.[23] The crystal structure of TiO_2 substrate is rutile as same as the high-temperature metal phase of VO_2. Since the *a*-axis length of VO_2 bulk is shorter than that of TiO_2 substrate with the lattice mismatch 0.863%, epitaxial VO_2 thin films receive tensile strain along the *a* axis, resulting in shortening the *c*-axis length. A V_2O_5 pellet was used as the target, which was obtained by milling V_2O_3 (99.9% pure) powder for an hour and then sintered at 773 K for 20 hours. After sintering, the samples were reground for 4 hours and then calcined at 683 K for 50 hours. The film thickness of VO_2 thin films was controlled ranging from 10 to 30 nm to investigate the effect of film thickness. The film thickness was measured by using surface profilometer. The deposition rate is 2.0 Å/min. After deposition, the films were cooled down to room temperature for 30 minutes under 1 Pa of the oxygen pressure. The crystal structures were evaluated by four-axis x-ray diffraction (XRD) measurement. The electrical properties of the films were measured by a four-probe method using physical property measurement system (PPMS; Quantum Design). The surface structures of the films were characterized by atomic force microscopy (AFM; Veeco DI3100 tapping mode). All measurements of XRD and AFM were performed at room temperature without thermal cycling. Subsequently the resistivity measurements were performed after heating up to 400 K. During the resistivity measurements the samples were thermally cycled in the temperature range between 400 and 200 K.

RESULTS AND DISCUSSION

Figure 1(a) shows the XRD patterns of VO_2 thin films grown on TiO_2 (001) single crystal substrate when varying the film thickness from 10 to 30 nm. Two significant peaks were observed over the range of film thickness. The lower angle peak is indexed to TiO_2 (002) and the other peak is due to VO_2 (002). The absence of other peaks indicates (001) oriented single phase. The epitaxy of the films is further confirmed by the reciprocal space map measurements around (112) peak as shown in Fig. 1(b). The *a*-axis length of films was fixed to that of TiO_2 substrate (0.4593 nm), indicating

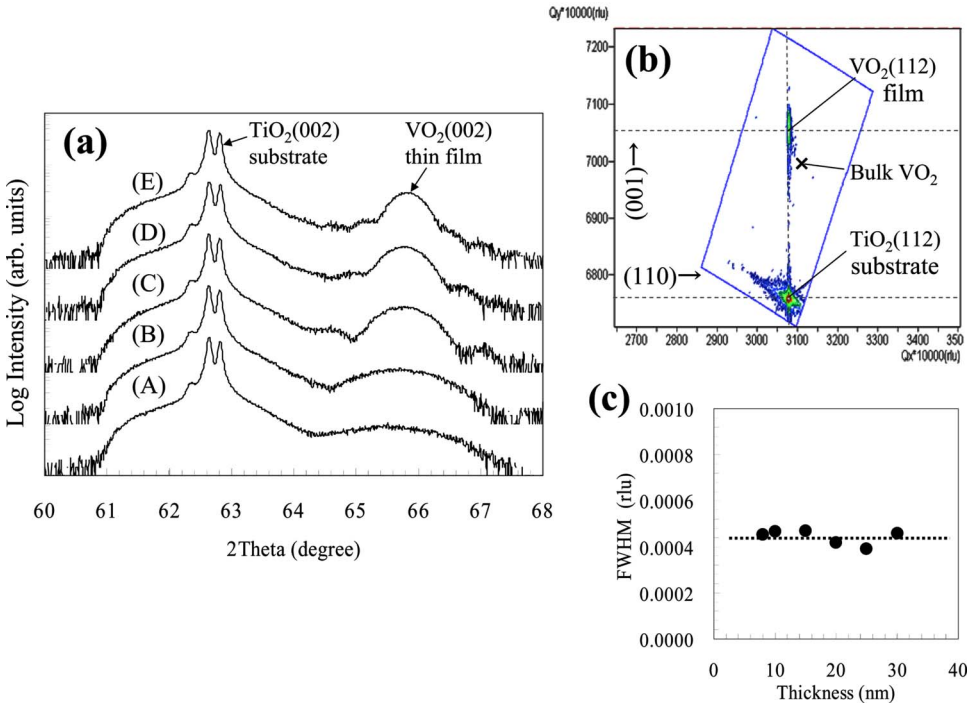

FIG. 1. (Color online) (a) XRD patterns of VO_2 thin films grown on TiO_2 (001) substrate with varying the film thickness. In the figure, (A) 10 nm, (B) 15 nm, (C) 20 nm, (D) 25 nm, (E) 30 nm, respectively. (b) Reciprocal space map data around the (112) peak. (c) Thickness dependence of the full width at half-maximum (FWHM) of in-plane axis at (112) peak.

the tensile strain effects on the epitaxial VO_2 thin films. The c-axis length of the film is calculated to be 0.2836 nm, which is shorter by 0.67% than that of bulk VO_2 c-axis length (0.2855 nm). Although the thinner films showed the broader (002) peaks in Fig. 1(a), such broadening is due to decreasing the total diffraction intensity with decreasing the film thickness. As seen in Fig. 1(c), the full width at half-maximum (FWHM) of in-plane axis at (112) peak was found to be insensitive to the film thickness variation, indicating that the film thickness variation does not affect the crystallinity of the films. In addition, as shown in Fig. 3 the observed abruptness of MIT for thinner films also indicates the well-crystallized structures since the abruptness is known to correspond to the crystallinity.[24] The film thickness dependence on both the a- and c-axis lengths is shown in Fig. 2. It can be clearly seen that both the a- and c-axis lengths are almost constant and insensitive to the film thickness variation. In other words, there was no observable strain relaxation within the range of this study at least on the XRD data. Since the c-axis length, i.e., V-V chain length, is known to influence strongly the transport properties of VO_2, especially the MIT temperature,[18–20] one can expect that the film thickness variation does not modify the transport properties.

Figure 3 shows the effect of the film thickness on the temperature dependence of the electrical resistivity. The MIT temperature for the films below 15 nm of the film thickness was around 300 K, which is much lower than that of bulk VO_2 (341 K), indicating the tensile strain effects as reported elsewhere.[19,20] Contrary to previous speculation based on XRD analysis, the transport properties including the resistivity and the MIT temperature were found to be very sensitive to the film thickness variation. The films below 15 nm thickness showed very abrupt single step MIT, indicating the single-phase nature, whereas the films above 15 nm tended to exhibit multisteps MIT. Surprisingly, the resistivity and the MIT temperature increased systematically with increasing the film thickness. As such, these trends on the transport properties clearly contradict to the absence of the film thickness dependence on the crystal structures observed by XRD. This discrepancy infers the presence of high resistive components within the films, which are not detectable by XRD.

Figure 4 shows the surface morphology AFM images of films when varying the film thickness. In the case of 10 nm film thickness, the flat surface was clearly observed—Fig. 4(a). On the other hand, the drastic change on the surface morphology above 15 nm film thickness was found as shown in Figs. 4(b) and 4(c). The line cracks were observed along with the directions of (100) and (010), reflecting the film epitaxy.[25] The line profile in the image reveals that the average width of line cracks is less than 10 nm. Above the criti-

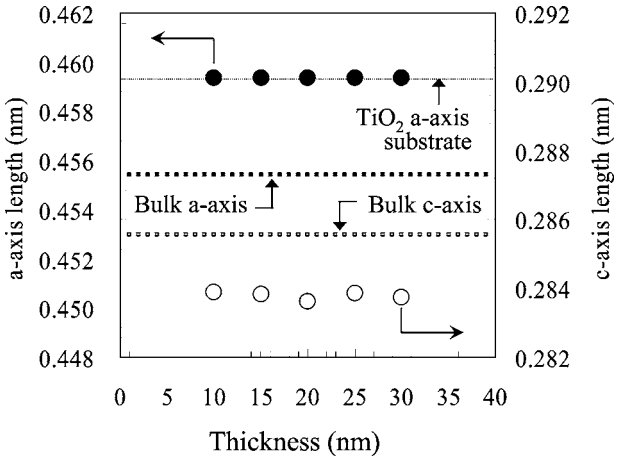

FIG. 2. Film thickness dependence on the a-axis length and the c-axis length of the films. The a-axis length of TiO_2 substrate, the a-axis length and the c-axis length of VO_2 bulk are also shown in the figure.

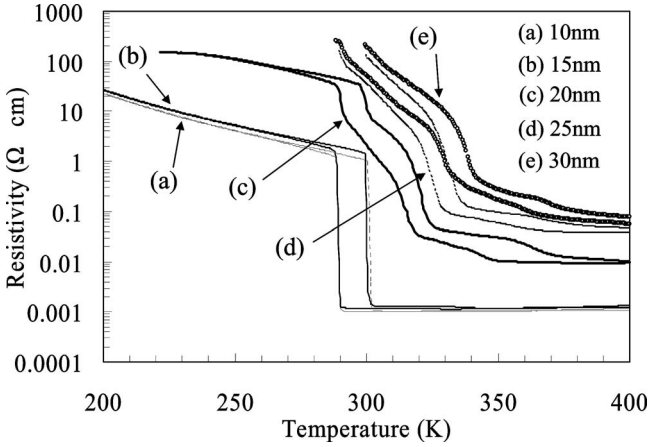

FIG. 3. Effect of film thickness variation on the temperature dependence of resistivity.

cal thickness 15 nm, a number of such line cracks increased systematically with increasing the film thickness as shown in Fig. 4(d). Thus there is the correlation between the change of transport properties and the nanoscale line cracks on the film thickness variation. Since the resistance in such line cracks is generally known to be very high,[26,27] the increase of the resistivity in Fig. 3 can be interpreted in terms of such high resistive components. In addition, the strain relaxation on the interface of line cracks tends to occur with increasing the film thickness.[28] After the formation of the line cracks, the surface stress should be partially released, leading to a different lattice constant. The stress relaxation should mainly appear at the interface of line cracks. Such local information was unfortunately not detectable by XRD technique because the total volume of crack surface areas is very small. It was estimated that the volume is approximately 1–2% of the entire film volume for the thickest film in this study. However,

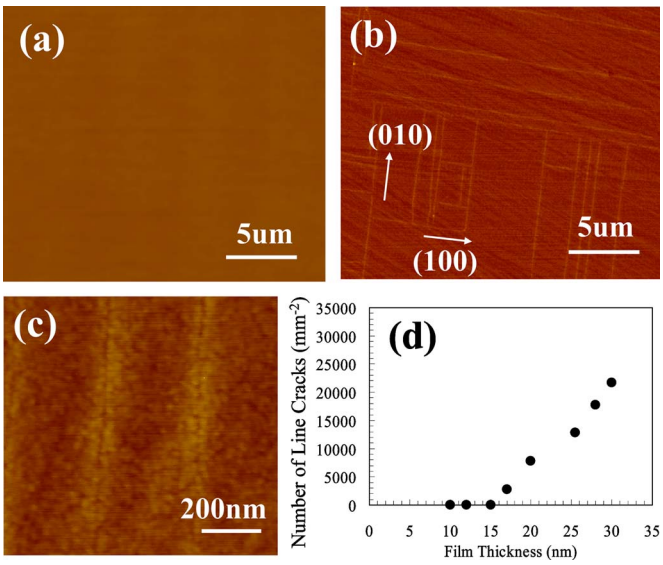

FIG. 4. (Color online) Surface morphology AFM images of films when varying the film thickness. (a) 10 nm data and (b) 30 nm data. (c) High-resolution AFM image of the selected area of line defects in (b).

when performing XRD measurement for much thicker film—60 nm, several relaxed c-axis lengths were detected on the XRD data. Thus a local stress relaxation on the interface of line cracks results in the multisteps MIT and also the systematic increase of MIT temperature with increasing the film thickness. One possible scenario for emerging the line cracks is a thermal stress relaxation during cooling process.[27] In fact, all trends, including the presence of the critical thickness and the increase of a number of line cracks, are qualitatively consistent with theoretical implications based on the thermal stress relaxation scenario.[27,28] According to fracture mechanics,[27,28] the critical film thickness t_{cr}, i.e., the threshold for crack propagation, can be described as $t_{cr}=0.5(k_f/\sigma)^2$, where k_f is the fracture toughness and σ is the tensile stress due to the different thermal expansions between the film and the substrate, which is given by $\sigma(T)=[E/(1-\nu)]\int_T^{T_d}[\alpha_f(T)-\alpha_s(T)]dT$, where E and ν are the Young's modulus and Poisson's ratio of the film, and α_f and α_s are the thermal expansion coefficients of the film and the substrate, respectively, and T_d stands for the temperature during deposition—643 K in this study. In the estimation of critical thickness t_{cr}, E and ν are of 200 GPa and 0.3,[27,29] and k_f is assumed to be 2.293 from the theoretical calculation of rutile structures.[30] If the temperature dependence of the thermal expansion coefficients is negligible for the temperature range between the deposition temperature (643 K) and MIT temperature (around 300 K in this study),[29] both α can be assumed to be constant, by taking α_f and α_s of 17.1 and $9.6(\times 10^{-6}\ \mathrm{K}^{-1})$, respectively.[31,32] However, in such estimation t_{cr} was overestimated to be 14.4 μm in comparison with the experimental value—15 nm. This is solely because the difference between VO_2 and TiO_2 in the thermal expansion coefficients is rather small. In fact the mechanical properties of both VO_2 and TiO_2 are very similar except for the MIT of VO_2.[29–33] Since the abrupt increase of α near MIT has been observed,[31] such effects should be incorporated in the estimation. By incorporating the data of α near MIT,[31] t_{cr} was calculated to be 15.9 nm, which is in good agreement with the experimental data—15 nm. Therefore the thermal stress relaxation via MIT is responsible for emerging the line cracks. Based on the formula of t_{cr}, larger k_f larger t_{cr}. Since

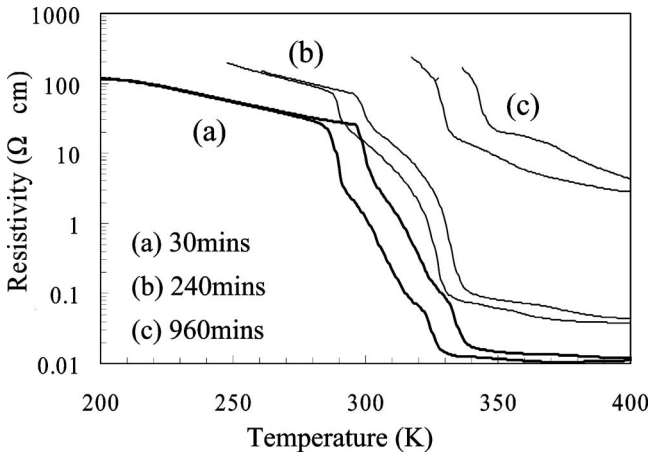

FIG. 5. Cooling time effects on the temperature dependence of resistivity.

it has been reported that the faster the cooling rate results in larger k_f,[34] it is interesting to investigate such effects on the transport properties of strained VO_2 thin films. Figure 5 shows the effect of the cooling time on the transport properties. The thickness of these films was controlled to be 20 nm. It can be clearly seen that the faster the cooling rate the lower the resistivity, indicating the suppression of the line cracks and also the controllability of emerging line cracks. Thus these experimental results highlight that the film thickness dependence of the transport properties is due to the nanoscale line cracks, and the thermal stress relaxation via MIT plays an important role on the transport properties of strained VO_2 thin films.

CONCLUSION

Strained oxide thin films exhibit a rich variety and controllability of the physical properties. A strain relaxation with varying the film thickness is known to affect significantly the properties. Here we investigate the transport properties of strained vanadium dioxide (VO_2) epitaxial thin films grown on TiO_2 (001) single crystal when varying the film thickness. When increasing the film thickness ranging from 10 to 30 nm, there were no significant changes on the crystal structures identified by x-ray diffraction, i.e., no observable strain relaxation effects. On the other hand, in electrical transport properties, increasing the film thickness resulted in not only emerging the multisteps of the metal-insulator transition (MIT) but also increasing the resistivity. The discrepancy between the observed crystal structure and the transport properties was related to the presence of the nanoscale cracks due to thermal stress. Thus controlling thermal stress relaxation via MIT rather than stress due to the lattice mismatch is essential to investigate the intrinsic nature on the transport properties of strained vanadium dioxide epitaxial thin films.

ACKNOWLEDGMENTS

The authors would like to acknowledge the Ministry of Education, Culture, Sports, Science and Technology of Japan for funding and supporting this project through the Center of Excellence (COE) program. The authors also acknowledge Dr. Kanai for his continuous advices.

*Corresponding author. Email address: yanagi32@sanken.osaka-u.ac.jp

[1] F. J. Morin, Phys. Rev. Lett. **3**, 34 (1959).
[2] M. W. Haverkort, Z. Hu, A. Tanaka, W. Reichelt, S. V. Streltsov, M. A. Korotin, V. I. Anisimov, H. H. Hsieh, H. J. Lin, C. T. Chen, D. I. Khomskii, and L. H. Tjeng, Phys. Rev. Lett. **95**, 196404 (2005).
[3] S. Biermann, A. Poteryaev, A. I. Lichtenstein, and A. Georges, Phys. Rev. Lett. **94**, 026404 (2005).
[4] Y. J. Chang, C. H. Koo, J. S. Yang, Y. S. Kim, D. H. Kim, J. S. Lee, T. W. Noh, Hyun-Tak Kim, and B. G. Chae, Thin Solid Films **486**, 46 (2005).
[5] K. Okazaki, H. Wadati, A. Fujimori, M. Onoda, Y. Muraoka, and Z. Hiroi, Phys. Rev. B **69**, 165104 (2004).
[6] M. Imada, A. Fujimori, and Y. Tokura, Rev. Mod. Phys. **70**, 1039 (1998).
[7] H. T. Kim, B. G. Chae, D. H. Youn, G. Kim, and K. Y. Kang, Appl. Phys. Lett. **86**, 242101 (2005).
[8] K. Y. Tsai, F. H. Wu, H. P. D. Shieh, and T. S. Chin, Mater. Chem. Phys. **96**, 331 (2006).
[9] M. Maaza, O. Nemraoui, C. Sella, A. C. Beye, and B. Baruch-Barak, Opt. Commun. **254**, 188 (2005).
[10] H. Wang, X. Yi, S. Chen, and X. Fu, Sens. Actuators, A **122**, 108 (2005).
[11] G. Xu, P. Jin, M. Tazawa, and K. Yoshimura, Sol. Energy Mater. Sol. Cells **83**, 29 (2004).
[12] G. Golan, A. Axelevitch, B. Sigalov, and B. Gorenstein, Microelectron. J. **34**, 255 (2003).
[13] K. Kato, P. K. Song, H. Okada, and Y. Shigesato, Jpn. J. Appl. Phys., Part 1 **42**, 6523 (2003).
[14] Z. Hiroi, T. Yamauchi, Y. Muraoka, T. Muramatsu, and J. Yamaura, J. Phys. Soc. Jpn. **72**, 3049 (2003).
[15] M. Takahashi, K. Tsukigi, E. Dorjpalam, Y. Tokuda, and T. Yoko, J. Phys. Chem. B **107**, 13455 (2003).
[16] L. A. L. de Almeida, G. S. Deep, A. M. N. Lima, and H. Neff, Appl. Phys. Lett. **77**, 4365 (2000).
[17] J. M. Gregg and R. M. Bowman, Appl. Phys. Lett. **71**, 3649 (1997).
[18] L. A. Ladd and W. Paul, Solid State Commun. **7**, 425 (1969).
[19] Y. Muraoka and Z. Hiroi, Appl. Phys. Lett. **80**, 583 (2002).
[20] Y. Muraoka, Y. Ueda, and Z. Hiroi, J. Phys. Chem. Solids **63**, 965 (2002).
[21] T. Kanki, H. Tanaka, and T. Kawai, Phys. Rev. B **64**, 224418 (2000).
[22] J. Zhang, H. Tanaka, T. Kanki, and T. Kawai, Phys. Rev. B **64**, 184404 (2000).
[23] K. Nagashima, T. Yanagida, H. Tanaka, and T. Kawai, J. Appl. Phys. **100**, 063714 (2006).
[24] E. Kusano and J. A. Theil, J. Vac. Sci. Technol. A **7**, 1314 (1989).
[25] C. H. Lei, G. Van Tendeloo, M. Siegert, J. Schubert, and Ch. Buchal, J. Cryst. Growth **222**, 558 (2001).
[26] C. A. Copetti, J. Schubert, W. Zander, H. Soltner, U. Poppe, and Ch. Buchal, J. Appl. Phys. **73**, 1339 (1993).
[27] Y. J. Tian, S. Linzen, F. Schmidl, A. Matthes, H. Schneidewind, and P. Seidel, Thin Solid Films **338**, 224 (1999).
[28] M. D. Thouless, J. Am. Ceram. Soc. **73**, 2144 (1990).
[29] F. C. Case, J. Vac. Sci. Technol. A **2**, 1509 (1984).
[30] D. Tromans and J. A. Meech, Minerals Eng. **15**, 1027 (2002).
[31] T. Kawakubo and T. Nakagawa, J. Phys. Soc. Jpn. **19**, 517 (1964).
[32] G. A. Samara and P. S. Peercy, Phys. Rev. B **7**, 1131 (1973).
[33] E. Francisco, M. Bermejo, V. García Baonza, L. Gerward, and J. M. Recio, Phys. Rev. B **67**, 064110 (2003).
[34] H. Baharav, B. Laufer, A. Mizrachi, and H. S. Cardash, J. Prosthet. Dent. **76**, 19 (1996).